Research Article

Markus Schindewolf*, Peter Németh, Ulrich Heber, Tiara Battich, Marcelo M. Miller Bertolami, and Marilyn Latour

Chemical fingerprints of He-sdO stars

Abstract: The chemical composition of helium-rich hot subluminous O stars plays an important role to understand and model their formation history. We present a spectroscopic analysis of four He-sdO stars, CD-31° 4800, [CW83] 0904-02, LSS 1274 and LS IV +10° 9. The analysis is based on archival optical and UV high-resolution spectra. We used Tlusty200/Synspec48 to compute line blanketed non-LTE model atmospheres and their corresponding synthetic spectra and derive the atmospheric parameters as well as the abundances of the most prominent elements. All stars have helium-dominated atmospheres with hardly any hydrogen and temperatures between 42000 K and 47000 K while their surface gravity spans between $\log g = 5.4$ and 5.7. CD-31° 4800 shows an enrichment of nitrogen and the characteristic pattern of hydrogen burning via the CNO-cycle, while the rest of the elements have about the solar abundance. This points to the slow merger of two helium white dwarfs as the most likely origin for this system. The other three stars are enriched in carbon, nitrogen and neon while their intermediate mass element's abundance scatters around the solar value. They were possibly formed in the deep mixing late hot flasher scenario.

Keywords: subdwarfs, abundances, He-sdO, hot flasher, slow merger, atmospheric parameters, stellar atmospheres

1 Introduction

Hot subdwarf stars (sdBs and sdOs) are core helium-burning stars with very thin hydrogen envelopes. They can be linked to late stages of the stellar evolution of low-mass stars. In a Hertzsprung-Russel diagram, they can be found between the main sequence and the white dwarf sequence. Subdwarf O-stars with helium dominated atmospheres are referred to as He-sdO stars.

He-sdO stars probably originate from a variety of evolutionary scenarios. In the merger scenario, two He-core white dwarfs in a binary system start to approach each other as the emission of gravitational waves leads to a shrinking orbit. At a certain point, the lighter companion is disrupted when it fills its Roche lobe. The debris forms an accretion disk and/or a hot corona around the more massive companion. Once helium is ignited in the core of the He-WD the remnant turns into a He-sdO star. Depending on the speed of accretion and the resulting temperature, thermonuclear reactions might alter the chemical composition of the debris. The slower the accretion, the lower the temperatures and the higher the chances that the original composition remains unaltered (Zhang & Jeffery 2012).

Another formation possibility is the late hot flasher scenario, which does not rely on binary evolution. If a low-mass star loses enough material on the red giant branch (RGB) before the helium core flash occurs, it descends along the hot white dwarf cooling track when a delayed core helium flash kicks in Castellani & Castellani (1993). A convection zone below the surface can push hydrogen to deeper layers where it is burnt during the He-flash. Depending on how deep the convection zone penetrates into the stellar interior, different amounts of hydrogen are burnt and different nuclear reactions occur, resulting in different chemical abundance patterns.

Determining the chemical abundances of He-sdO stars is an important task as they are directly linked to their formation history. There are three different classes of He-sdO stars, according to their chemical composition: carbon-rich, nitrogen-rich and those enriched in both carbon and nitrogen (Hirsch 2009; Stroer et al. 2007). The chemical composition of the atmospheres of He-sdO stars can be used as a testbed for different evolutionary scenarios. In addition, it becomes easier to pick chemically peculiar

Corresponding Author: Markus Schindewolf: Dr. Karl-Remeis Sternwarte, Sternwartstraße 7, 96049 Bamberg, Germany; Email: Markus.Schindewolf@fau.de

Peter Németh, Ulrich Heber, Marilyn Latour: Dr. Karl-Remeis Sternwarte, Sternwartstraße 7, 96049 Bamberg, Germany

Tiara Battich: Instituto de Astrofísica de La Plata, CONICET-UNLP, Argentina; Facultad de Ciencias Astronómicas y Geofísicas, UNLP, Argentina

Marcelo M. Miller Bertolami: Instituto de Astrofísica de La Plata, CONICET-UNLP, Argentina

stars and those sticking out from the classical three categories. In this work we present a complete Non-Local Thermodynamic Equilibrium (NLTE) analysis of four He-sdO stars, including all important metals for evolutionary models, including iron and nickel.

2 Methods

We used Tlusty200 and Synspec48 to calculate model atmospheres and synthetic spectra. The model atmospheres covered complete NLTE conditions and line-blanketing with the most detailed model atoms available on the corresponding websites. For fitting the observational data, the Spectrum Plotting and Analysis Suite (SPAS) was applied (Hirsch 2009). This program uses a spline fit to interpolate between the different model spectra and a downhill simplex algorithm for determining the errors (see (Napiwotzki et al. 2004) for details).

Before addressing the metal abundances of the sample stars, the procedure to determine the atmospheric parameters with H/He grids was inspected in more detail. Pure H/He grids without additional metals have been widely used for the analysis of several subdwarf stars. Before applying them to stars it was necessary to check if they are adequate enough to reproduce the stellar atmosphere and especially the temperature stratification correctly. A model atmosphere was set up at an effective temperature of T_{eff} = 47000 K, log(g)=5.7 and n(He)=100×n(H) and the stratification as a function of the optical depth was derived. Afterwards, metals were added in NLTE conditions with abundances matching those in [CW83] 0904-02. The added metals are C, N, O, Ne, Mg, Al, Si, P, S , Fe and Ni. The stratification was determined for a HHeC, a HHeCNO, an atmosphere with all the intermediate mass elements and an atmosphere with all available elements. The result can be seen in figure 1, where the atmosphere with iron and nickel serves as a reference point for the temperature stratification.

It can be clearly seen that a pure HHe atmosphere shows drastic deviations concerning the temperature stratification when compared to more metal-rich atmospheres. In the important line forming region, the differences in temperature reach up to 3000 K. By just adding one metal (carbon) at the appropriate (high) abundance, the deviations are decreased dramatically to around 500 K. More metals hardly make any difference in the line forming region when compared to the atmosphere with iron and nickel. As the computation time increases with the number of included elements, adding one metal seems to be the

best trade-off between accuracy and time consumption. As an additional crosscheck, we used the final model atmosphere of CD -31° 4800 and the resulting synthetic spectrum as a mock spectrum and fitted it with a HHeN grid, tailored to the nitrogen content of CD -31° 4800. The input atmosphere had the following atmospheric parameters:

- T_{eff}=42200 K
- log(g)=5.60
- log(n(He)/n(H))=2.61

The fit resulted in the following parameters.

- T_{eff} = 42900 ± 400 K
- log(g)=5 , 60 ± 0.03
- log(n(He)/n(H))=2.61(fix)

By fixing the helium abundance and applying the fitting procedure we can reproduce the atmospheric parameters of the mock spectrum almost exactly. The offset in effective temperature (700 K) matches the predictions from the stratification analysis (∼500 K) very well.

It was therefore decided to apply the procedure of determining the atmospheric parameters with a HHe+metal grid for all the sample stars. In practice, a first set of atmospheric parameters was determined with a pure H/He grid and a model atmosphere with these parameters was set up. From this model atmosphere, a small subgrid was calculated to determine the carbon or nitrogen abundance of the star, depending on whether it belongs to the C-rich or the N-rich class. Afterwards, the HHe grid was updated with the corresponding metal at the correct abundance and the atmospheric parameters were re-determined.

After the final atmospheric parameters were set up, the abundances for the other metals were derived. From a model atmosphere with the parameters from the HHe+metal grid, all elements (except helium of course) were set to solar abundance. Small subgrids were computed for each individual metal one after the other to fit the available spectral lines. The fit was a simultaneous fit of several isolated lines. The model atmosphere was then updated with the resulting abundance and the next element was fitted. In a first run, only the available optical spectra were fitted and iron and nickel were not included in the calculations. This was done to get a first estimate of the chemical composition and to save computation time on the long run. Following the analysis of the intermediate mass elements, iron and nickel were included with abundances determined from UV spectra. After this step, all elements (except helium) were refitted from optical and UV spectra simultaneously. The resulting abundances are the error weighted abundances from optical and UV data.
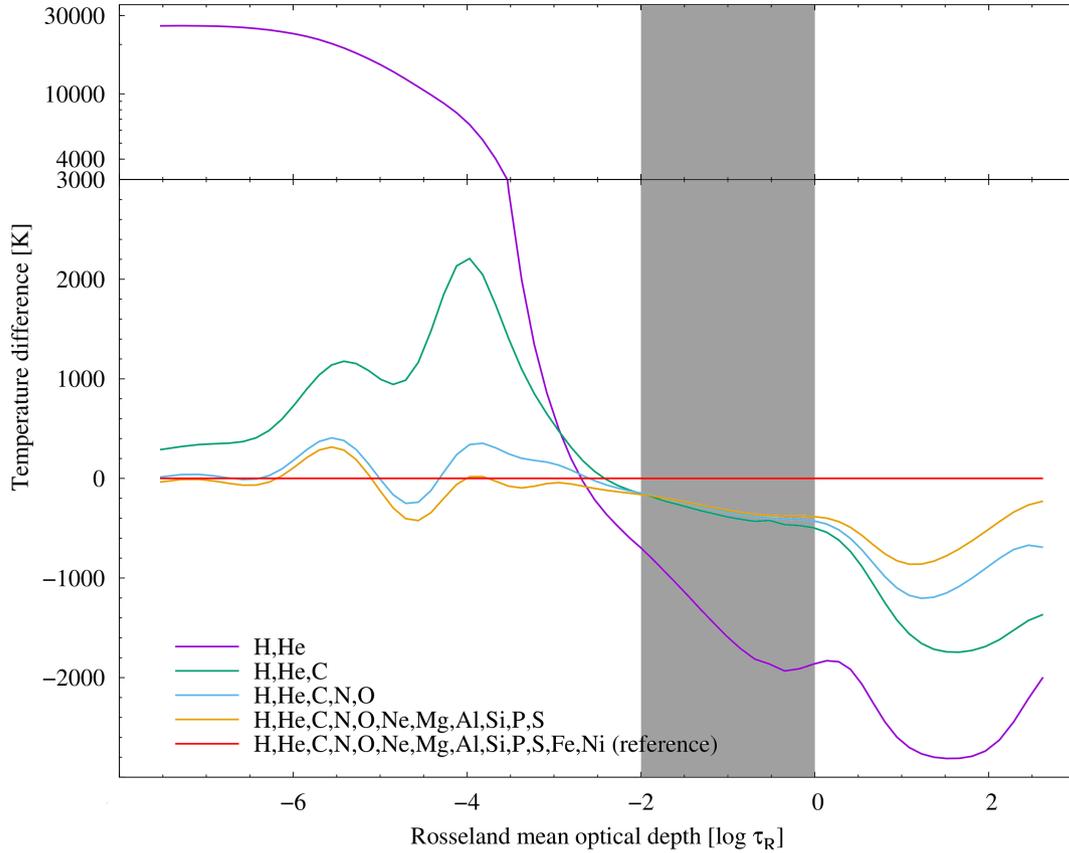
Figure 1. Temperature stratification of different NLTE atmospheres. The atmosphere containing iron and nickel was used as a reference point. The region of line formation is marked by the gray bar.

Table 1. Information about the sample stars analyzed in this work.

Star	Instrument	Wavelength range [Å]	R
CD -31° 4800	UVES	3281...4562	68642
*	UVES	4583...6686	107200
*	IUE	1150...1980	10000
*	IUE	1850...3350	10000
*	FORS1	3400...5900	1700
[CW83] 0904-02	FEROS (2x)	3527...9216	48000
*	FUSE (2x)	900...1190	22000
*	IUE (3x)	1150...1970	10000
LSS 1274	UVES (2x)	4726...6835	66320
*	UVES (2x)	3024...3884	49620
*	FUSE (2x)	900...1190	22000
LS IV +10° 9	UVES	3281...4562	53750
*	IUE (2x)	1150...1980	10000

3 Results

The stars analyzed in this work are CD -31° 4800, LSS 1274, [CW83] 0904-02and LS IV +10° 9. Table 1 lists information about the different stars and their spectra analyzed during this work. Optical high-resolution Echelle spectra were taken from the European Southern Observatory (ESO) Data Archive and UV spectra (IUE and FUSE) from the Mikulski Archive for Space Telescopes (MAST).

The data from the UVES spectrograph were particularly useful as it covered the optical-UV, a region where a large amount of Ne II lines can be found.

In Table 2 an overview on the atmospheric parameters of the four sample stars are given. They were determined by using the HHe+metal grids, tailored to the carbon or nitrogen abundances of the corresponding stars.

While CD -31° 4800, LSS 1274 and LS IV +10° 9 show no significant rotation ($v_{rot\,sin(i)} < 5\,km\,s^{-1}$) the projected rotational velocity is $35 \pm 4\,km\,s^{-1}$ for [CW83] 0904-02. The rotational broadening is clearly visible in both optical and UV data. Figure 2 shows several carbon lines from the FUSE spectrum with the best fit in red and the line profiles without rotation in green, demonstrating that the rotation is obvious.
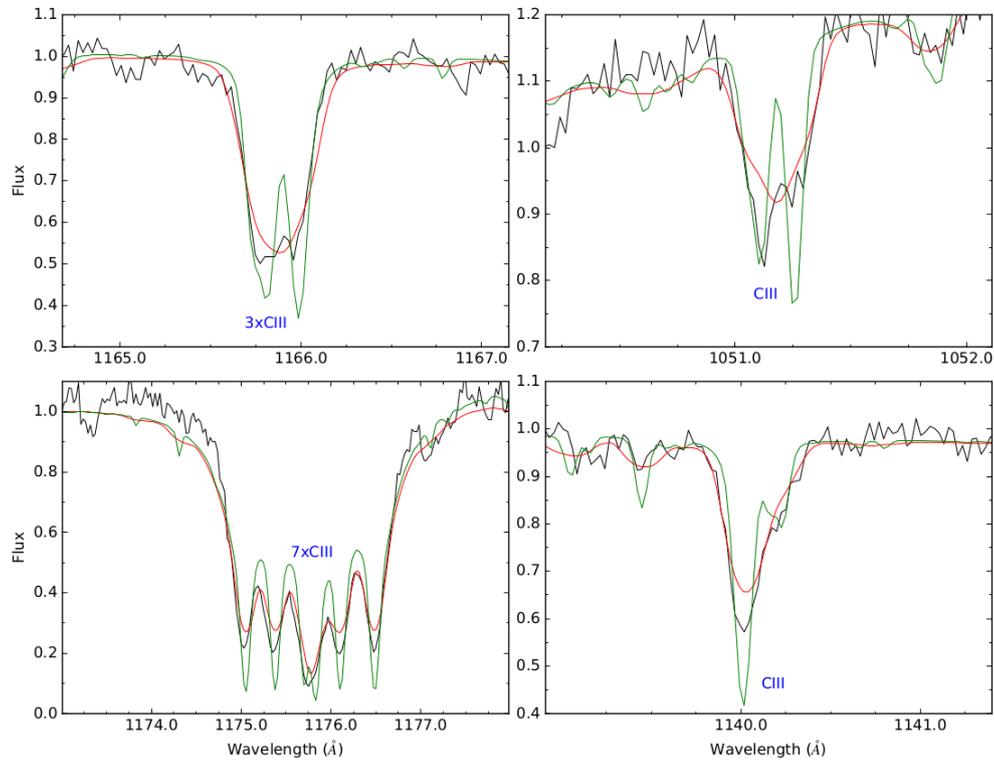
Figure 2. Fit of carbon lines in the FUSE spectrum of [CW83] 0904-02 (red) and line profiles without rotation (green).
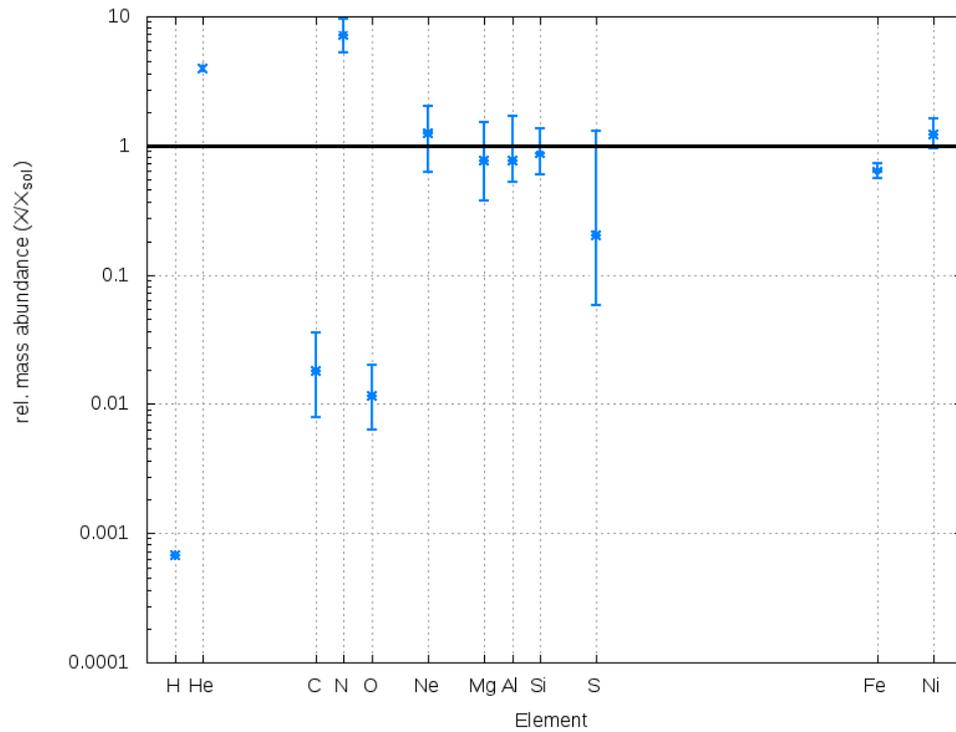

Figure 3. Abundance pattern of CD -31° 4800. Given is the relative mass abundance compared to the sun. The solar value is indicated by the black line.
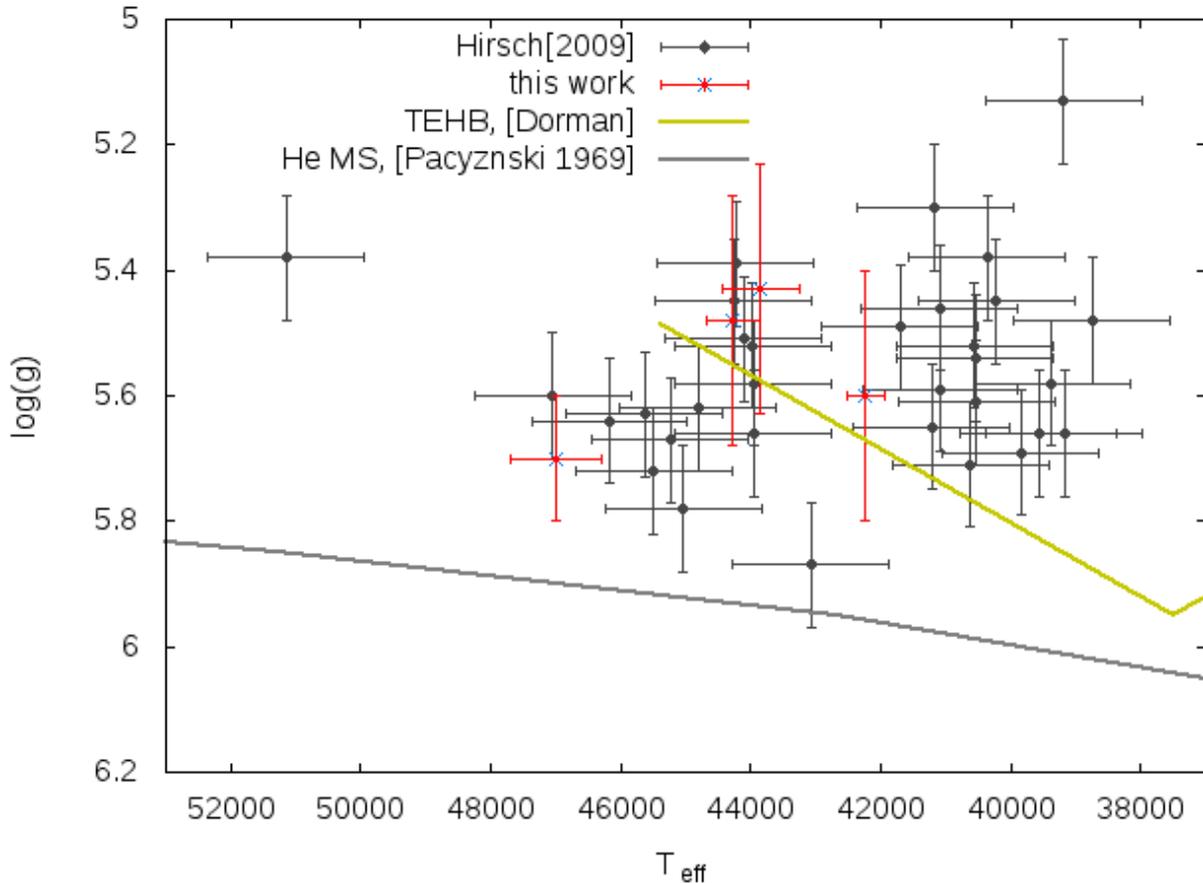
Figure 4. T_{eff}/log(g) diagram of sample stars in comparison with He-sdOs from Hirsch[2009]. In addition, tracks for the He-Main Sequence and the Termina Age Extreme Horizontal Branch are shwon.

Table 2. Atmospheric parameters for the four sample stars, determined from HHe+metal grids.

Star	T_{eff}	log(g)	log(n(He)/n(H))
CD -31° 4800 (N)	42200 ± 300	5.60 ± 0.15	2.61 ± 0.20
LSS 1274 (CN)	44300 ± 400	5.48 ± 0.20	2.17 ± 0.25
LS IV +10° 9 (CN)	43900 ± 200	5.43 ± 0.15	2.73 ± 0.25
[CW83] 0904-02 (CN)	47000 ± 500	5.70 ± 0.20	2.00 ± 0.30

The atmospheric parameters are typical for He-sdO stars. Figure 4 shows their position in a T_{eff}/log(g) diagram in comparison with other He-sdO stars taken from (Hirsch 2009).

In table 3, the logarithmic mass abundances for each element in the sample stars are listed as the originated from the fits. The last column gives the solar mass abundance as a reference (Asplund et al. 2009). If no value is given for a specific element, either no spectral lines could be found or the fit did not reproduce the spectral lines well enough and was therefore rejected.

It is apparent that CD -31° 4800 is strongly enriched in nitrogen and depleted in carbon and oxygen while the other three stars are all enriched in carbon, nitrogen and neon but to a different extend. Figure 3 and figure 5 illustrate the abundance patterns of CD -31° 4800 and the three other stars respectively. Given is the relative mass abundance for each element with respect to the solar mass abundance.

4 Discussion

The derived abundance patterns allow us to draw direct conclusions regarding the formation history of the corresponding stars. Figure 6 shows the position of the sample stars in a log(T_{eff})/log(g) diagram in combination with two evolutionary tracks. The red track represents the shallow
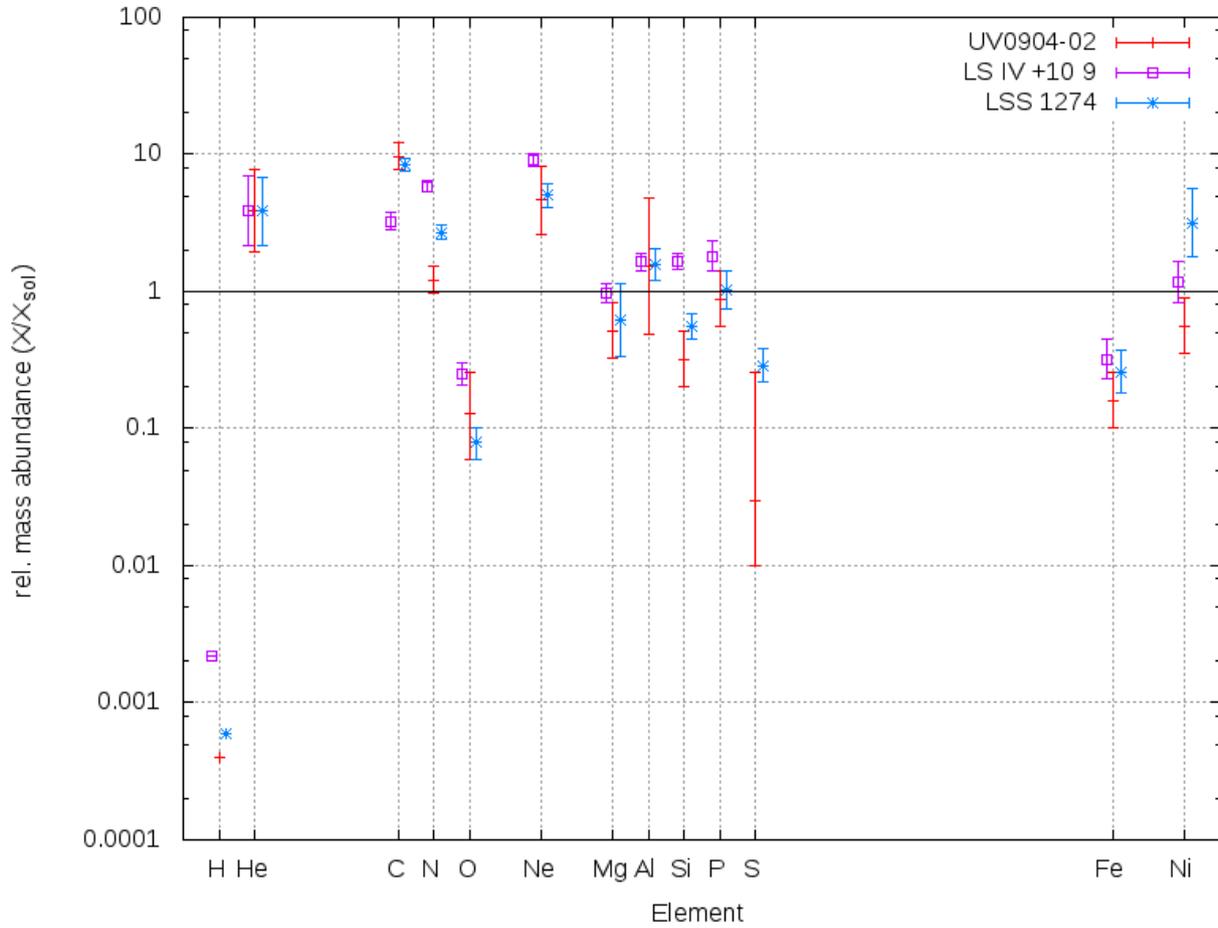
Figure 5. Abundance pattern of CN-rich He-sdO stars.Given is the relative mass abundance compared to the sun. The solar value is indicated by the black line.

Table 3. Logarithmic surface mass abundances of the analyzed elements. Hydrogen was the reference element in the calculations of the model atmospheres, no errors are given for hydrogen. The last column gives the solar mass abundances taken from (Asplund et al. 2009) as a reference.

|	CD -31° 4800	LSS 1274	[CW83] 0904-02	LS IV +10° 9	solar
H	−3.21	−2.79	−2.62	−2.79	−0.13
He	0.00 ± 0.20	−0.02 ± 0.25	−0.02 ± 0.30	−0.01 ± 0.25	−0.6 ± 0.01
C	−4.46 ± 0.20	−1.69 ± 0.05	−1.65 ± 0.10	−2.11 ± 0.15	−2.62 ± 0.05
N	−2.39 ± 0.10	−2.75 ± 0.05	−3.07 ± 0.10	−2.39 ± 0.04	−3.16 ± 0.04
O	−4.21 ± 0.20	−3.39 ± 0.10	−3.13 ± 0.29	−2.84 ± 0.11	−2.24 ± 0.05
Ne	−2.91 ± 0.20	−2.23 ± 0.10	−2.23 ± 0.26	−1.94 ± 0.05	−2.90 ± 0.10
Mg	−3.42 ± 0.30	−3.37 ± 0.27	−3.43 ± 0.15	−3.16 ± 0.07	−3.15 ± 0.05
Al	−4.63 ± 0.19	−4.01 ± 0.14	−4.07 ± 0.51	−4.04 ± 0.08	−4.25 ± 0.04
Si	−3.19 ± 0.14	−3.44 ± 0.10	−3.67 ± 0.34	−2.96 ± 0.07	−3.17 ± 0.03
P	–	−5.22 ± 0.14	5.28 ± 0.20	−4.98 ± 0.13	−5.23 ± 0.03
S	−4.51 ± 0.44	−4.04 ± 0.10	−5.03 ± 0.17	–	−3.50 ± 0.03
Fe	−3.32 ± 0.09	−3.48 ± 0.10	−3.68 ± 0.25	−3.38 ± 0.11	−2.89 ± 0.04
Ni	−4.46 ± 0.16	−3.64 ± 0.12	−4.41 ± 0.20	−4.08 ± 0.15	−4.15 ± 0.04
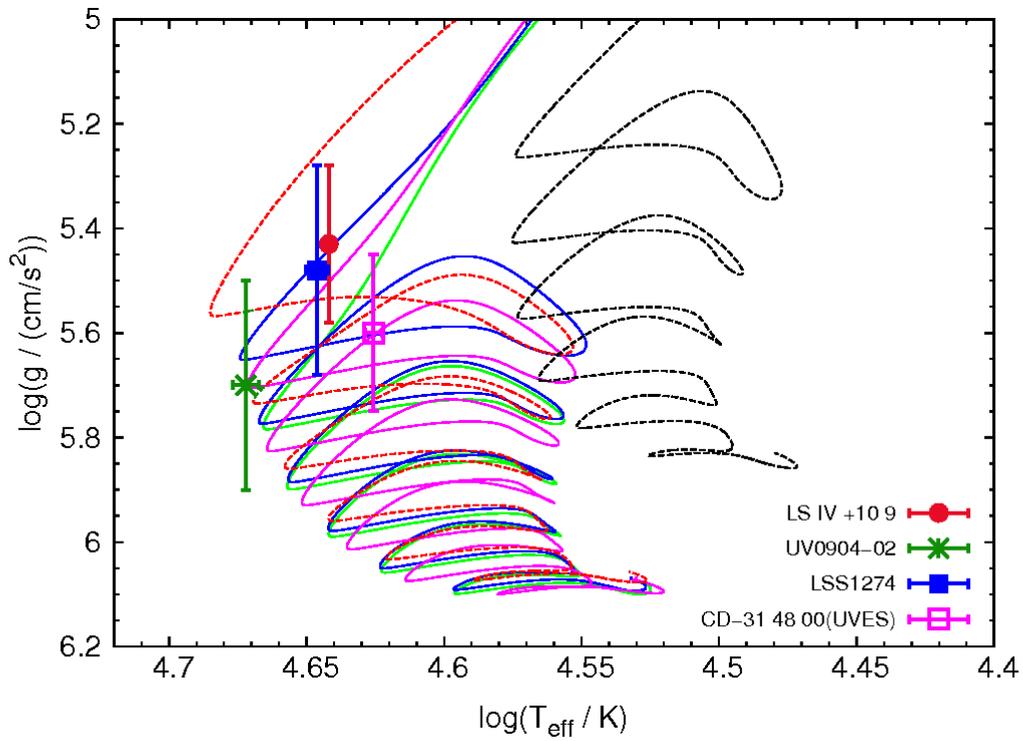
Figure 6. Kiel diagram with evolutionary tracks for deep mixing and different stellar masses (red, blue, green and purple) and shallow (black dashed) mixing hot flasher scenarios.
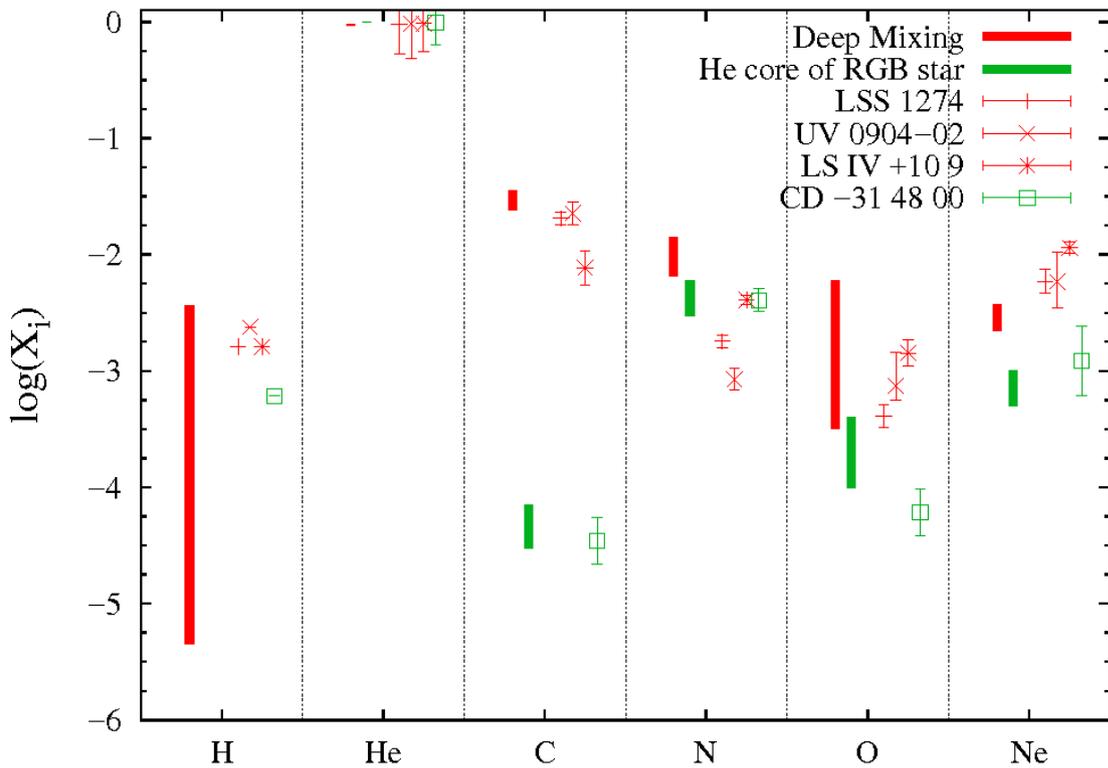

Figure 7. Abundance predictions from deep-mixing hot flasher (Battich) and slow merger models (Miller-Bertolami).

mixing scenario while the black one stands for the deep mixing hot flasher scenario. It is obvious that the shallow mixing case can be ruled out for all stars, while the hot flasher case seems possible for all of them.

In figure 7 predictions of mass abundances are shown, resulting from models for the deep mixing hot flasher case [(Battich et al. 2018), submitted.].

Concerning LSS 1274, [CW83] 0904-02 and LS IV $+10°$ 9, the predicted nitrogen abundance is a bit too high, neon seems to be too strongly enriched in the stars. This can be explained by the shortcomings of one dimensional modeling and may be solved when three dimensional modeling becomes available. The hydrogen, helium, carbon and oxygen abundances are in good agreement with the model predictions for the deep-mixing late hot flasher case. We also compared the abundance patterns of these three stars to the predictions of a composite merger model (Zhang & Jeffery 2012). None of them shows an abundance pattern that is consistent with the model predictions for these cases.

For CD $-31°$ 4800 the mass abundance predictions from the deep mixing hot flasher are not compatible with the measurements. However, the slow merger of two He-core WDs seems more likely (Zhang & Jeffery 2012). In figure 7 the green bars represent the predicted chemical composition of the He core of a RGB star. As the slow merger scenario does not alter the chemical composition of the material, the predicted abundances are usable for a comparison with the slow merger case. For all elements, the measured mass abundances of CD $-31°$ 4800 are in good agreement with the model predictions. However, the projected rotation velocity of CD $-31°$ 4800 is smaller than 5km s^{-1}. This calls the merger scenario for CD $-31°$ 4800 into questions. Modelling of the angular momentum loss during and past the merger is necessary to clarify this issue.

References

Asplund, M., Grevesse, N., Sauval, A. J., and Scott, P. 2009, ARA&A, 47, 481–522.

Battich, T., Miller Bertolami, M. M., Córsico, A. H., & Althaus, L. G., 2018, arXiv:1801.07287.

Castellani, M. and Castellani, V. 1993, ApJ, 407, 649–656.

Hirsch, H. 2009, Hot Subluminous Stars: On the Search for Chemical Signatures of their Genesis, Friedrich-Alexander University Erlangen-Nürnberg, Erlangen, Germany.

Napiwotzki, R., Yungelson, L., Nelemans, G., Marsh, T. R., Leibundgut, B., Renzini, R. et al. 2004, ASP Conference Series, In: R. W. Hilditch, H. Hensberge and K. Pavlovski, Spectroscopically and Spatially Resolving the Components of the Close Binary Stars (20-24 October 2003, Dubrovnik, Croatia), 318, 402–410.

Stroeer, A., Heber, U., Lisker, T., Napiwotzki, R., Dreizler, S., Christlieb, N., and Reimers, D. 2007, A&A, 462, 269–280.

Zhang, X. and Jeffery, C. S. 2012, MNRAS, 419, 452–464.